Automatic Quantification of Histological Studies in Allergic Asthma

Mónica Abella,[1] José Manuel Zubeldia,[2] Laura Conejero,[2†] Norberto Malpica,[3] Juan José Vaquero,[1] Manuel Desco[1*]

[1]Laboratorio de Imagen, Unidad de Medicina Experimental. Hospital Gregorio Maranón, Madrid, Spain

[2]Servicio de Alergia, Unidad de Medicina Experimental. Hospital Gregorio Maranón, Madrid, Spain

[3]Laboratorio de Análisis de Imagen Médica, Universidad Rey Juan Carlos, Móstoles Madrid, Spain

†Current address: Immunology Unit, Department of Infectious and Tropical Diseases, London School of Hygiene and Tropical Medicine, London, United Kingdom.

Received 12 February 2008; Revision Received 15 July 2008; Accepted 18 August 2008

Preliminary results were presented as a poster at the 2006 Workshop Microscopic Image Analysis with Applications in Biology and at the XXVI European Academy of Allergology and Clinical immunology Congress.

Additional Supporting Information may be found in the online version of this article.

Contract grant sponsor: CD TEAM project, CENIT program, Ministerio de Industria

*Correspondence to: Manuel Desco, Laboratorio de Imagen, Unidad de Medicina Experimental. Hospital Gregorio Maranón, C/ Doctor Esquerdo, 46, 28007 Madrid, Spain

Email: desco@mce.hggm.es

Abstract

The evaluation of new therapies to treat allergic asthma makes frequent use of histolog ical studies. Some of them are based on microscope observation of stained paraffin lung sections to quantify cellular infiltrate, an effect directly related to allergic processes. Currently, there is no software tool available for doing this quantification automatically. This paper presents a methodology and a software tool for the quantification of cellular infiltrate in lung tissue images in an allergic asthma mouse model. The image is divided into regions of equal size, which are then classified by means of a segmentation algo rithm based on texture analysis. The classification uses three discriminant functions, built from parameters derived from the histogram and the co occurrence matrix. These functions were calculated by means of a stepwise discriminant analysis on 79 samples from a training set. Results provided a correct classification of 96.8% on an independ ent test set of 251 samples labeled manually. Regression analysis showed a good agree ment between automatic and manual methods. A reliable and easy to implement method has been developed to provide an automatic method for quantifying micros copy images of lung histological studies. Results showed similar accuracy to that pro vided by an expert, while allowing analyzing a much larger number of fields in a repea table way.

Key terms

microscopy; lung tissue; allergic asthma; co occurrence matrix; image analysis; segmen tation; texture

Asthma is a chronic inflammatory disease of the lung, characterized by airway hyperresponsiveness to a variety of stimuli, eosinophilic inflammation of the airways, mucus hypersecretion, and elevated serum IgE levels (1). Mortality of asthma has increased worldwide, despite the use of currently available medications, underlining the need for the development of novel therapies (2 4).

Previous studies indicate that murine models are useful for studying allergic dis eases, including certain aspects of bronchial asthma such as cellular tissue inflamma tion and pulmonary function. Three studies are commonly performed in this type of experiments to assess the effects: immunologic parameters (immunoglobulines and cytokines), pulmonary function (bronchial hyperactivity), and histological studies (cellular infiltrate and bronchial mucus secretion). The latter are currently assessed by visual inspection by an expert, as there is no automatic analysis tool available. Such a tool would speed up the process, also providing a more repeatable quantification.

In theory, the amount of cellular infiltrate could be accurately assessed by means of an appropriate segmentation algorithm (i.e., border detection) identifying each cell nucleus on the image. The main difficulty for this individual cell segmentation arises from the existence of cell aggregates, which hinders the detection of the con tours. This is a difficult task for most image processing algorithms and the authors do not know of any previous successful attempt. Furthermore, the nuclei of cells in the bronchial wall are similarly stained and have the same size, making it difficult to

differentiate them from the cellular infiltrate. The classical segmentation by thresholding also proved to be not sufficient to separate the cellular infiltrate areas. It can be observed, however, that the infiltrate has a texture pattern different from other regions in the image. This fact suggested applying region identification based on texture analysis (5).

Methods based on texture analysis have been used successfully to detect structural alterations in patients with Sjogren Larsson syndrome (6), quantify necrosis in cell cultures (7), for automated migration analysis (8), to segment intravascular ultrasound (9), to identify neoplastic nuclei by characterizing chromatin structure in breast tumors (10,11) and in prostate cancer (12), to segment chromatin regions (13), and for monitoring tumor cell viability during treatment with an antivascular drug (14).

This paper presents a method for the automatic quantification of cellular infiltrate in histological studies of the lung based on texture analysis. Texture parameters have been extracted from a set of training samples, calculating the optimum discriminant functions by stepwise procedures. The method and its validation against manual quantification are presented. Preliminary results of this work were presented previously (15,16).

Methods and Results

Segmentation is based on the classification of each region of the image into one of three a priori classes, based on a vector of texture parameters. These texture parameters were previously obtained from the luminance component of the images in a training data set by means of a stepwise discriminant analysis that also provided the corresponding discriminant (Fisher) functions. We developed a software tool that makes use of these functions to implement an automatic parameter extraction and classification. This tool also generates a mask of the tissue area (non air) and provides the final result in terms of percentage of cellular infiltrate area over total tissue area and severity scores.

The overall procedure followed in this work is depicted in Figure 1. Each box of the flowchart is explained in the following sections.

Study Acquisition and Preparation

Induction of systemic allergic response was achieved by the subcutaneous administration of *Olea europaea* extract in BALB/c mice. Allergic airway response was generated by transnasal instillation of the allergens. For histological analysis, lungs were fixed in 4% paraformaldehyde PBS and tissue blocks were embedded in paraffin. Ten micrometer sections were stained with Hematoxilyn Eosin (17).

We acquired the images with an Olympus CK40 microscope at 10× magnification, and captured them with an Olympus DP11 camera adapted to the microscope. Then images of size 1712 × 1368 (0.50 μm pixel size) were transferred to a PC for analysis.

The extraction of texture features was performed on the luminance component, as it conveys enough information to identify the textures selected. The image was down sampled

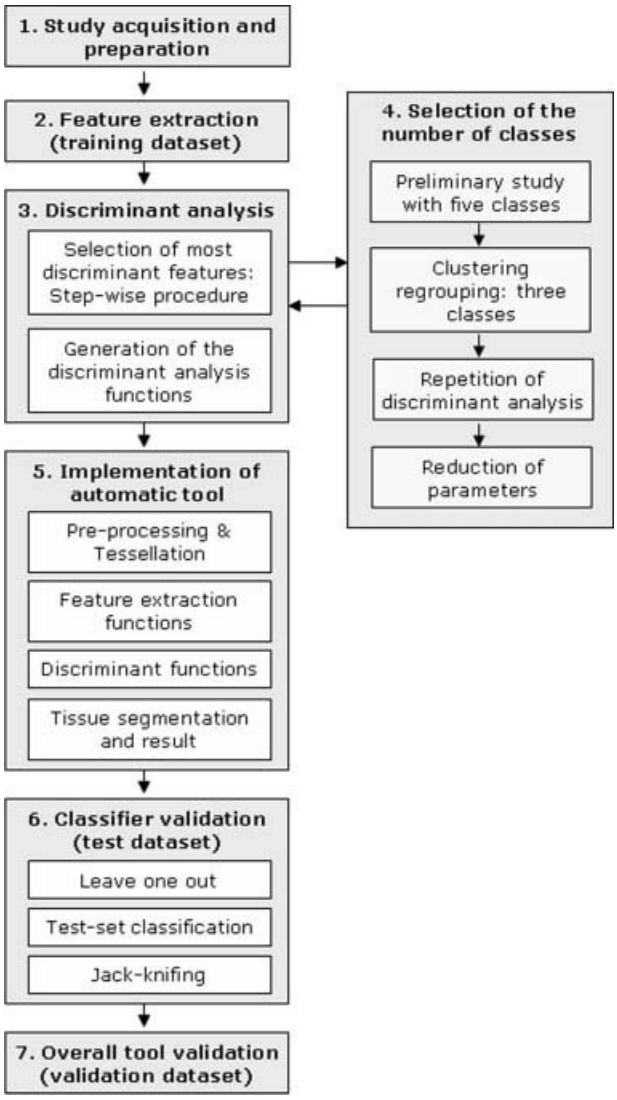

Figure 1. Flow chart of the overall procedure.

by a factor of 4 and a median filter with a 7 point mask was applied to eliminate impulsive noise.

Total number of images used was 30, divided into two groups:

- 9 images for training and testing the classifier. We obtained 330 samples from these images to build the dataset: 79 samples used for training and 251 samples for testing the classifier.
- 21 images with different percentages of infiltrate area for validation of the complete tool.

Feature Extraction and Classification

Texture parameters used in this application can be classified into first order statistics, computed from the normalized histogram, and second order statistics, computed using the Gray Level Co occurrence matrix (GLCM) for distances of 1 5 pixels and angles of 0°, 90°, 180°, and 270° with a prequantization of 5 bits per pixel (18). These parameters were extracted

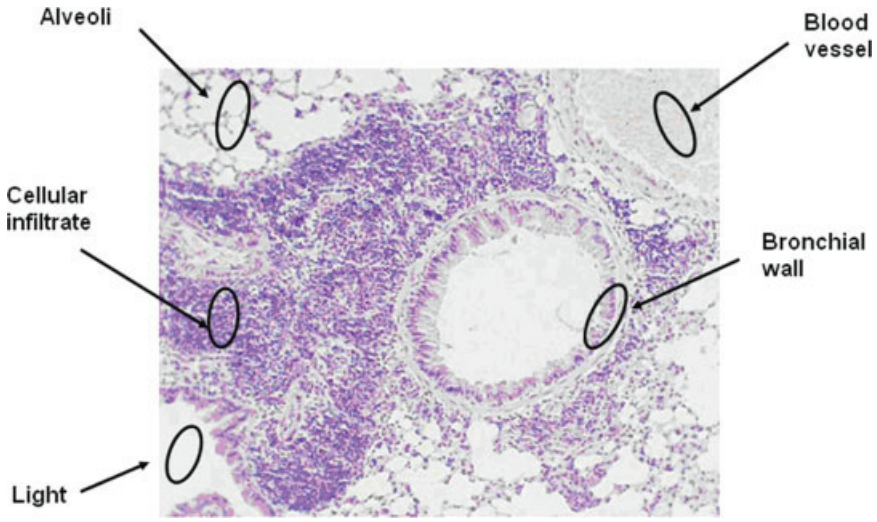

Figure 2. Image of a 10 μm lung section stained with Hematoxilyn Eosin showing the existence of inflammatory infiltrate in the lung. The five textures identified in lung studies are shown (''light,'' ''cellular infiltrate,'' ''alveoli,'' ''blood vessel,'' and ''bronchial wall''). [Color figure can be viewed in the online issue, which is available at www.interscience.wiley.com.]

using MaZda (an acronym derived from "Macierz Zdarzen," the Polish term for "co occurrence matrix"), a software tool developed at the Institute of Electronics, Technical University of Lodz, Poland (19,20). As a result, we obtained 229 parameters for each sample (9 from the normalized histogram and 220 from the 20 Co occurrence matrices mentioned above). The final result for the 79 samples in the training set was a table of 79 $\times$ 229 parameter values.

Discriminant Analysis

Given the amount of data generated, a reduction of dimensionality of the feature vector was clearly advisable. This reduction was performed by selecting the most discriminant features by means of a stepwise discriminant analysis based on the Fisher criterion. At each step, the procedure included the feature that better contributed to class separation, following the criterion of maximization of the Mahalanobis distance between the two closest groups (21). An inclusion condition, based on an F test, was used to evaluate if the change in discrimination was significant. The F to enter and F to remove values used were 3.84 and 2.71, respectively. This analysis was performed with SPSS for Windows, Rel. 11.5.1. (SPSS, Chicago).

Selection of the Number of Classes

The lung histological sections can be separated into five distinct textures, highlighted in Figure 2. These were chosen as the five initial classes for the texture based classification, and

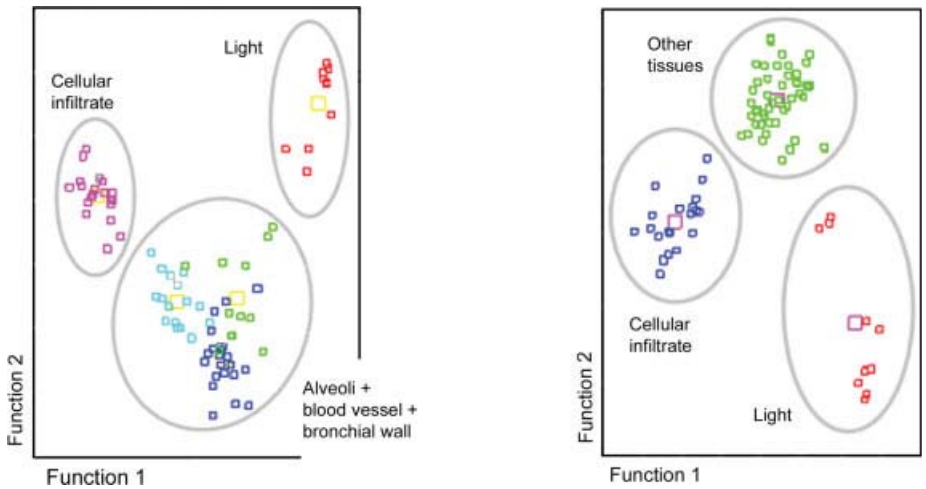

Figure 3. Left: Five clusters obtained with the stepwise discriminant analysis for five classes on the training set (79 samples). Function 1 and Function 2 are the result of computing the two most discriminant functions. The figure shows a possible cluster regrouping by making a new class from ''blood vessel,'' ''alveoli,'' and ''bronchial wall,'' denoted ''other tissues.'' Right: Final clusters obtained after cluster regrouping and parameter reduction (using only seven parameters). [Color figure can be viewed in the online issue, which is available at www.interscience.wiley.com.]

each of the samples in the training dataset was manually classi fied by an expert into one of those classes.

Left panel of Figure 3 shows the resulting five clusters of samples as a function of the result of computing the first and second discriminant functions. It can be noticed that there are three main groups, which suggests a possible cluster regroup ing. This approach is further supported by the fact that our goal is just to quantify the infiltrate area, thus not being neces sary to separately identify each one of the five classes.

As a result of this preliminary study, we decided to reduce the number of classes to three: "cellular infiltrate," "bronchial lumen," and "other tissues" (new class including "blood ves sels" "alveoli," and "bronchial wall").

Samples belonging to the new "other tissues" class where relabeled and the discriminant analysis was repeated. The new stepwise discriminant analysis resulted in the selection of 13 texture parameters shown in Table 1.

Considering the relatively high number of parameters obtained from the stepwise process, we decided to study the effect of eliminating the less significant ones i.e., those included in the last steps. To this end, we eliminated the less significant parameters one by one and repeated the leave one out analysis while the classification success was maintained within acceptable values (final value of 97.5% of correct classi fication vs. the initial value of 100%). The final number of pa rameters was 7, whose names and weighting coefficients for the three linear discriminant functions are shown in Table 2. The number of parameters satisfied the well known rule of thumb of not including more than one independent variable per 10 cases approximately (there were 79 samples in the training data set). The reduction in the number of parameters led to a reduction of 31% in processing time.

Resulting clusters as a function of the result of computing the two main discriminat functions are presented in the right panel of Figure 3.

Table 1. Parameters entered and removed during the definitive stepwise procedure after clustering regrouping (three classes)

STEP	ENTERED	REMOVED
1	Inverse difference moment (2,0)	
2	Entropy of sum (5,5)	
3	Entropy of difference (1,0)	
4	Correlation (3,0)	
5	2nd order angular moment (5, 5)	
6	Percentile 01%	
7	Percentile 99%	
8		Correlation (3,0)
9	Percentile 90%	
10	2nd order angular moment (5,0)	
11	2nd order angular moment (1,0)	
12	Correlation (1,1)	
13	Sum of squares (0,4)	
14	Correlation (0,1)	

This stepwise discriminant analysis resulted in the selection of 13 texture parameters. For explanation of the parameters, see the online Supporting Information.

Table 2. Seven most discriminant parameters and their coefficients for the three linear Fisher functions

	CELLULAR INFILTRATES	WALL	OTHER TISSUES
Percentile 01%	10.272	9.814	9.573
Percentile 90%	7.430	7.271	7.647
Percentile 99%	0.951	1.026	1.608
Entropy of diff (1,0)	10 113.489	10 179.965	9919.718
Inv diff moment (2,0)	9006.342	9099.251	8734.140
Entropy of sum (5,5)	3141.666	3047.379	2945.159
Angular moment (5, 5)	2878.253	2755.525	2691.116
(Constant)	6408.611	6367.628	5946.772

For explanation of the parameters, see the online Supporting Information.

Implementation of the Automatic Tool[1]

Once the specific texture parameters were selected and the discriminant functions were known, we implemented an automatic tool to perform the whole quantification process using IDL 6.2 (Research Systems, Boulder, CO). This software tool tessellates the images, calculates the texture parameters for each region, and applies the discriminant functions (22) obtained in the previous phase following a process similar to the one described in (7). Images are divided into regions of $w_c \times w_c$ (w_c 55) pixels, denoted as "classification window," whose size determines the resolution of the classification. Each region is assigned to a class on the basis of the texture parame ters computed from a wider region of $w_a \times w_a$ pixels, denoted as "analysis window" (Figure 4, top left).

The size of the classification window, w_a, was heuristically selected to achieve a reasonable trade off between resolution and speed. To this end, we repeated the complete discriminant analysis using four different window sizes and compared the individual classification results with those provided by the leave one out validation (see section "Classifier Validation" for details) in order to assess the stability of the results for each window size. The best results were obtained with w_a 85.

The classification process proceeds by moving the analysis window in steps of size w_c, leading to an overlapping of w_c w_a pixels between two contiguous windows. The final results are expressed as the percentage of the total tissue area that corre sponds to infiltrate. The total tissue area is obtained by thresh olding the hue component of the image (Figure 4, top right).

Classifier Validation

A leave one out method was used to obtain an initial estimate of the correct classification rate. This method involves leaving out each case in turn, calculating the functions based on the remaining cases, and then classifying the left out case. The leave one out method yielded a classification success rate of 97.5% on the training set.

A more accurate estimate of the correct classification rate was derived by classifying a test dataset of 251 samples not

[1]The automatic tool is available under request at: mabella@mce.hggm.es.

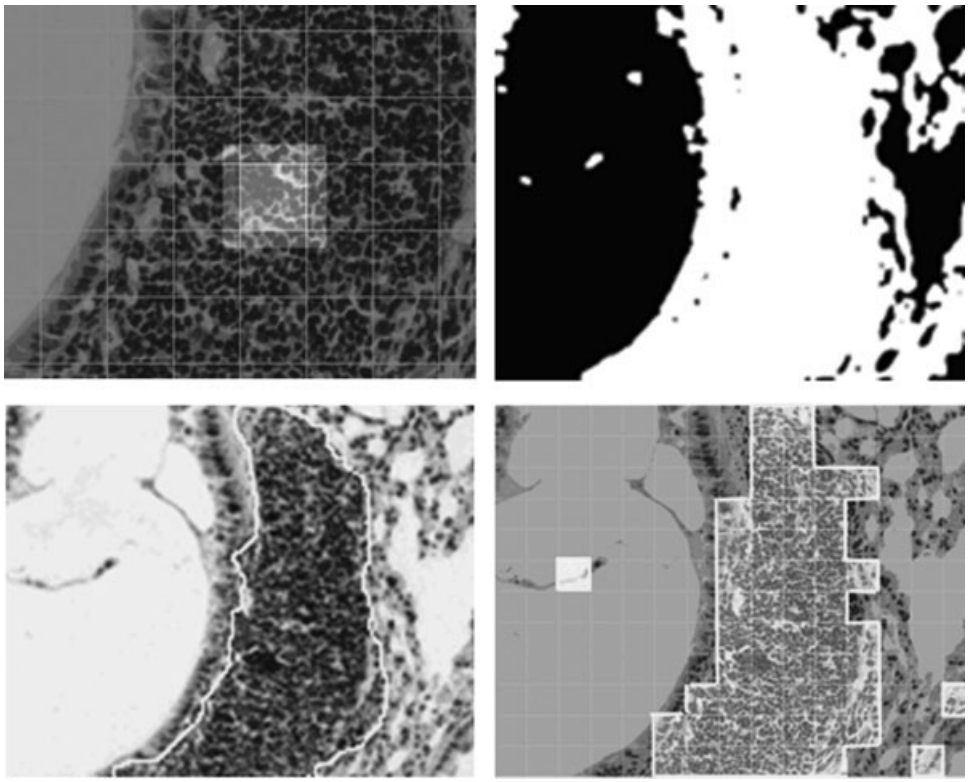

Figure 4. Top: Analysis window (brighter square) and classification window (grid) overlapped on an image (left) and tissue mask in white (right). Bottom: Manual segmentation overlapped on the analyzed image (left) and automatic segmentation overlapped on the analyzed image (right).

included in the training set. Results on the test set showed a classification success of 96.8%.

The robustness of the discriminant functions was also assessed by jack knifing: 10% of samples were randomly taken out and the discriminant functions were estimated from the remaining data in five different runs.

Overall Tool Validation

Finally, to assess the usefulness of the complete quantifi cation tool, we compared results provided by the automatic method with those measured manually by an expert on 21 new images which specifically corresponded to cases at differ ent stages of the disease.

Currently, there is no consensus on how to quantify this kind of studies, and many different scores or grades have been proposed, thus hindering any objective comparison. For this reason, we created a gold standard based on manual segmenta tion. To this end, an expert segmented all the images by manu ally delimiting the infiltrate area (Figure 4, bottom left) and labeled them with a severity score defining four categories ran ging from no inflammation (Score I) to maximum severity (Score IV). Infiltrate percentage was obtained by dividing the manually segmented infiltrate area by the tissue mask area, similarly to what is done in the automatic method.

We compared the infiltrate percentage values obtained with manual and automatic methods by means of a regression analysis. This regression analysis showed a good agreement between automatic and manual methods (Figure 5, top left).

The top right panel of Figure 5 shows the scatter plot of infiltrate percentages versus severity scores. From this figure, it is easy to establish the thresholds that better separate the dif ferent score categories. To compare the results in terms of se verity scores, these category limits set by the expert were trans lated into the range of values provided by the automatic method by means of the regression curve previously obtained. The degree of concordance in terms of severity scores was measured by the kappa coefficient.

The result of the comparison of manual and automatic severity scores is presented in Figure 5, bottom. Only one mis match can be observed between types III and IV, yielding a concordance coefficient (kappa) of 0.87.

The tool has been tested on an Intel Pentium, 3 GHz with 1GB RAM. For images of size 825 $\times$ 660, average classification time was 15 s. Almost 60% of the time was dedicated to the computation of the Co occurrence matrix. An example of the result obtained is shown in Figure 4, bottom right.

Discussion

This work presents an approach for the automatic quanti fication of microscopy images of histological lung studies. This type of studies, very common in the research of allergic asthma and other pulmonary diseases, are currently performed by simple visual inspection of the images. Classification results

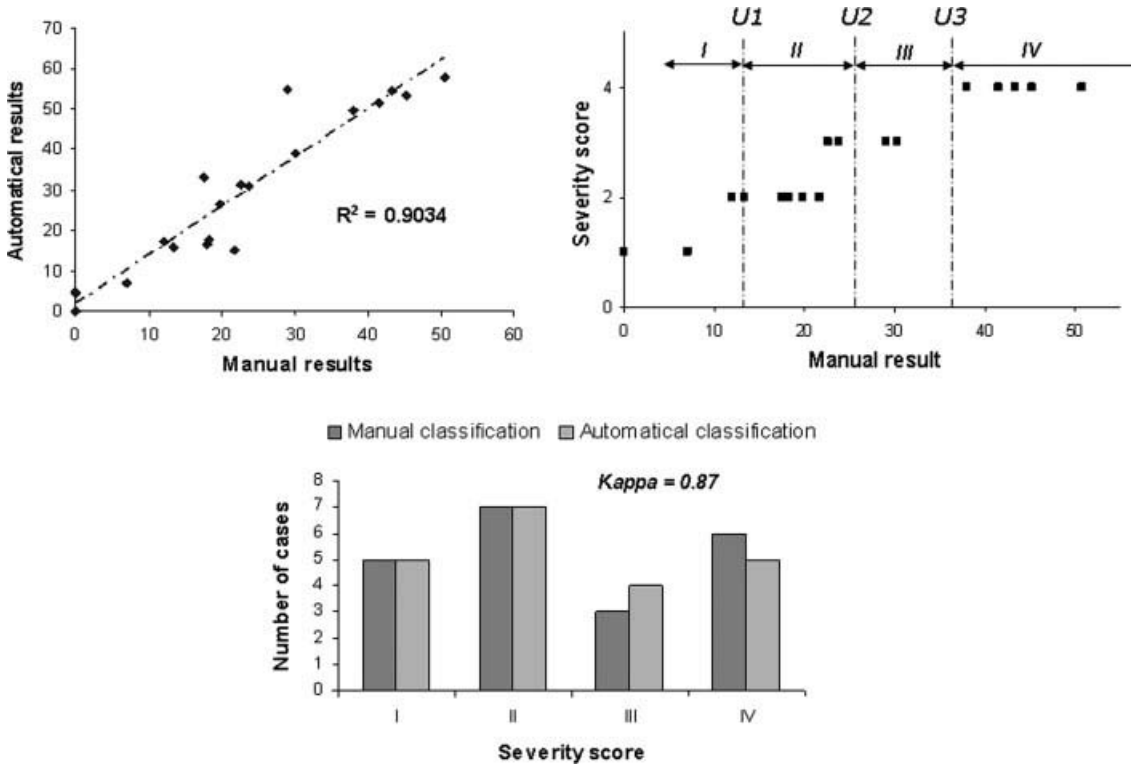

Figure 5. Top left: Regression analysis of the infiltrate percentage measured with the automatic tool vs. manual results. Top right: Definition of the severity score categories. Thresholds were set from the manual results. Bottom: Global classification results according to severity score.

obtained by our procedure are promising (96.8% accuracy) in a reasonable time (15 sec per image of size 825 × 660).

We obtained a very good agreement with manual results (R^2 0.9). One of the possible causes for the differences between the automatic and manual results may be the partial volume effect, as manual segmentation is made on a pixel by pixel basis, whereas automatic segmentation is obtained with lower resolution on windows of 55 × 55 pixels.

The analysis window size was fixed and empirically deter mined. It must be large enough to have a sufficient number of pixels for parameter computing. The size of the classification window determines the resolution of the classification. Using a smaller window increases the resolution (minimizing partial volume effect) but also the computational burden.

The method presented uses only first and second order statistics, computed from the normalized histogram and from the co ocurrence matrices. These parameters are easy to obtain and require a short processing time.

Regarding processing time, the slowest stage in the quan tification process is the texture feature extraction algorithm. The processing time could be reduced by reprogramming and optimizing the code in lower level programming languages. However, we considered the processing time achieved as ade quate, and it would only be a concern if the study included a very high number of images.

The number of parameters in the discriminant functions was reduced to seven, based on the classification results obtained with the leave one out method. A more exhaustive study, measuring the marginal discrimination power provided by the last parameters included, would have been advisable. Nevertheless, for end users, the success rate achieved constitutes a reasonable trade off between processing time and accuracy.

Although the individual algorithms and techniques used are well established, we have proposed a combination of dif ferent steps and a selection of particular algorithms to better achieve a reliable quantification of lung histological studies, resulting in an automatic tool for quantification. A methodol ogy similar to ours could be used to segment and classify other types of histological studies. To that end, steps 1 3 in the flow chart would have to be repeated to compute the most discri minant texture features, and the new discriminant functions for each particular case. The software tool should be modified to include the new texture features and discriminant functions obtained. These changes are straightforward because of the modularity of the implementation.

In summary, a reliable and easy to implement method has been developed to provide an automatic method for quan tifying microscopy images of lung histological studies. Results showed similar accuracy to that provided by an expert, while enabling the analysis of a much larger number of fields in an objective and repeatable way.

Acknowledgments

The authors thank the Institute of Electronics, Technical University of Lodz (Poland), for providing the MaZda texture analysis software, in the framework of the EU COST B11 project.

Literature Cited

1. Tortora G, Grabowski S. Principles of Anatomy and Physiology. New York: Wiley; 2002.
2. D'Amato G, Liccardi G, D'Amato M, Cazzola M. Outdoor air pollution, climatic changes and allergic bronchial asthma. Eur Respir J 2002;20:763–776.
3. Wills-Karp M. Murine models of asthma in understanding immune dysregulation in human asthma. Immunopharmacology 2000;48:263–268.
4. Holt P, Sly P, Martinez F, Weiss S, Bjorksten B, von Mutius E, Wahn U. Drug development strategies for asthma: In search of a new paradigm. Nat Immunol 2004;5:695–698.
5. Haralick RM, Shanmugam K, Dinstein I. Textural features for image classification. IEEE Trans Syst Man Cybernetics 1973;3:610–621.
6. Auada MP, Adam RL, Leite NJ, Puzzi MB, Cintra ML, Rizzo WB, Metze K. Texture analysis of the epidermis based on fast Fourier transformation in Sjogren-Larsson syndrome. Anal Quant Cytol Histol 2006;28:219–227.
7. Malpica N, Santos A, Tejedor A, Torres A, Castilla M, Garcia-Barreno P, Desco M. Automatic quantification of viability in epithelial cell cultures by texture analysis. J Microsc 2003;209:34–40.
8. Qin J, Chittenden TW, Gao L, Pearlman JD. Automated migration analysis based on cell texture: Method & reliability. BMC Cell Biol 2005;6:9.
9. Mojsilovic A, Popovic M, Amodaj N, Babic R, Ostojic M. Automatic segmentation of intravascular ultrasound images: a texture-based approach. Ann Biomed Eng 1997;25:1059–1071.
10. Weyn B, van de Wouwer G, van Daele A, Scheunders P, van Dyck D, van Marck E, Jacob W. Automated breast tumor diagnosis and grading based on wavelet chromatin texture description. Cytometry 1998;33:32–40.
11. Wouwer VD, Weyn, Scheunders, Jacob, Marck V, Dyck V. Wavelets as chromatin texture descriptors for the automated identification of neoplastic nuclei. J Microsc 2000;197:25–35.
12. Yogesan K, Jorgensen T, Albregtsen F, Tveter KJ, Danielsen HE. Entropy-based texture analysis of chromatin structure in advanced prostate cancer. Cytometry 1996;24:268–276.
13. Beil M, Irinopoulou T, Vassy J, Wolf G. A dual approach to structural texture analysis in microscopic cell images. Comput Methods Programs Biomed 1995;48:211–219.
14. Chen G, Jespersen S, Pedersen M, Pang Q, Horsman MR, Jorgensen HS. Evaluation of anti-vascular therapy with texture analysis. Anticancer Res 2005;25:3399–3405.
15. Abella M, Zubeldia JM, Conejero L, Malpica N, Vaquero JJ, Desco M. Preliminary results on automatic quantification of histological studies in allergic asthma. In: Metaxas DN, Whitaker RT, Rittscher J, Sebastian TB, editors. Proceedings of 1st Workshop on Microscopic Image Analysis with Applications in Biology (in conjunction with MICCAI, Copenhagen); 2006. pp 50–54.
16. Conejero L, Abella M, Vaquero J, Baeza M, Varela-Nieto I, Desco M, Zubeldia J. Automatic quantification of airway inflammation on histological images with a new software tool. Allergy 2007;62:475.
17. Conejero L, Higaki Y, Baeza ML, Fernández M, Varela-Nieto I, Zubeldia JM. Pollen-induced airway inflammation, hyper-responsiveness and apoptosis in a murine model of allergy. Clin Exp Allergy 2007;37:331–338.
18. Sonka M, Hlavac V, Boyle R. Image Processing, Analysis and Machine Vision. Great Britain: University Press; 1993.
19. Materka A, Strzelecki M. Texture Analysis Methods—A Review. Poland: Technical University of Lodz; 1998. p COST B11 report (presented and distributed at MC meeting and workshop in Brussels, June 1998).
20. Szczypinski PM, Strzelecki M, Materka A. MaZda A Software for Texture Analysis. International Symposium on Information Technology Convergence, 2007. p 245–249.
21. Dillon W, Goldstein M. Multivariate Analysis: Methods and Applications. New York: Wiley; 1984.
22. Duda R, Hart P, Stork D. Pattern Classification, 2nd ed. New York: Wiley; 2001.